JOURNAL OF THERMOPHYSICS AND HEAT TRANSFER
Vol. 20, No. 4, October–December 2006

Lattice Boltzmann Method Applied to Variable Thermal Conductivity Conduction and Radiation Problems

Nishant Gupta,* G. Raghu Chaitanya,† and Subhash C. Mishra‡
Indian Institute of Technology Guwahati,
Guwahati 781 039, India

DOI: 10.2514/1.20557

In the present article, application of the lattice Boltzmann method has been extended to solve the energy equation of a problem involving temperature dependent thermal conductivity. To validate the formulation, transient heat conduction in a planar medium with and without temperature dependent thermal conductivity was analyzed. Next, a problem involving transient conduction and radiation in a participating medium was considered. To compare with the performance of the lattice Boltzmann method, the energy equation was also solved using the finite difference method. The discrete ordinates method was used to compute the radiative information in both methods. After benchmarking the results against those available in the literature, temperature and heat flux results in the two methods were compared for different parameters. The results of the two methods were found to compare very well.

Nomenclature

c_p	=	specific heat, $(\mathrm{kJ/kg}) \cdot \mathrm{K}$
e_i	=	propagation speed in the direction i in the lattice, $\lvert \boldsymbol{e}_i \rvert$, m/s
$\boldsymbol{e}_i$	=	propagation velocity in the direction i in the lattice, m/s
f_i	=	particle distribution function in the i-direction, K
$f_i^{(0)}$	=	equilibrium particle distribution function in the i-direction, K
G	=	incident radiation, $\mathrm{W/m^2}$
I	=	intensity, $\mathrm{W/m^2}$
k	=	thermal conductivity, $(\mathrm{W/m}) \cdot \mathrm{K}$
M	=	number of lattices/control volumes
m	=	index for direction
N	=	conduction-radiation parameter, $k_0\beta/4\sigma T_W^3$
q	=	heat flux, $\mathrm{W/m^2}$
S	=	source term, $\mathrm{W/m^3}$
T	=	temperature, K
t	=	time, s
w	=	weight
X	=	length of the medium, m
x	=	length, m
x^*	=	nondimensional length, βx
α	=	thermal diffusivity, $\mathrm{m^2/s}$
β	=	extinction coefficient, $\mathrm{m^{-1}}$
γ	=	coefficient for thermal conductivity variation
γ'	=	variable thermal conductivity parameter, $(\mathrm{W/m}) \cdot \mathrm{K^2}$
δ	=	polar angle
ε	=	emissivity
θ	=	nondimensional temperature
κ_a	=	absorption coefficient, $\mathrm{m^{-1}}$
μ	=	direction cosine with respect to the x-axis
ξ	=	nondimensional time, $\alpha\beta^2 t$
ρ	=	density, $\mathrm{kg/m^3}$
σ	=	Stefan–Boltzmann constant, 5.67×10^{-8} $(\mathrm{W/m^2}) \cdot \mathrm{K^4}$
σ_s	=	scattering coefficient, $\mathrm{m^{-1}}$
τ	=	relaxation time, s
Φ	=	phase function
Ψ	=	nondimensional heat flux
ω	=	scattering albedo
Ω	=	rate of change of f_i due to collision, K/s

Subscripts

b	=	boundary
C	=	conductive
E, W	=	east, west
i	=	direction
n	=	index for the lattice node
P	=	cell center
R	=	radiative
T	=	total
0	=	reference
1, 2	=	directions in a D1Q2 lattice

Superscripts

m	=	direction
*	=	nondimensional quantity

I. Introduction

IN the recent past, the usage of the lattice Boltzmann method (LBM) as an alternative to the conventional computational fluid dynamics (CFD) solvers has gained momentum [1–15]. As a different approach from CFD, the LBM has been demonstrated to be successful in simulations of a large class of problems in science and engineering [1–4]. The proponents of the LBM consider this method to have the potential to become a versatile CFD platform [1–5].

Traditional CFD techniques such as the finite element method, the finite difference method (FDM), and the finite volume method are top-down approaches that solve the macroscopic transport equations of mass, momentum, and energy by directly discretizing them. The LBM, on the other hand, is a bottom-up approach that uses kinetic equation models and corresponding relations between the actually simulated statistical dynamics at a microscopic level and transport equations at the macroscopic level. By construction, the approach of the LBM assures conservation of relevant macroscopic quantities such as mass and momentum. The LBM inherits many of the advantages of molecular dynamics and kinetic theories due to its

Received 16 October 2005; revision received 12 April 2006; accepted for publication 27 April 2006.

*Undergraduate student, Department of Mechanical Engineering.
†Undergraduate student, Department of Mechanical Engineering.
‡Professor, Department of Mechanical Engineering; Corresponding author, scm_iitg@yahoo.com.

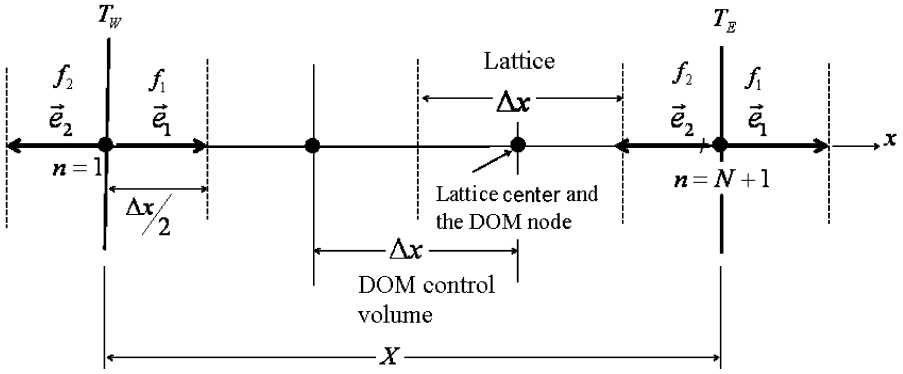

Fig. 1 One-dimensional planar geometry under consideration. Lattices and control volumes are staggered.

microscopic origin. In comparison with conventional CFD methods, the advantages of the LBM include, among others, a simple calculation procedure, a simple and efficient implementation for parallel computation, and an easy and robust handling of complex geometries. The LBM is second-order accurate in both space and time [1].

The applicability of the LBM in fluid mechanics is well established [1–8]. Currently, its application to heat transfer is also gaining momentum [9–15]. Quite recently, the LBM has been applied to solve a hyperbolic heat conduction problem [11] and phase-change problems [14,15]. Mishra and Lankadasu [11] and Mishra et al. [12] used the LBM to solve the energy equations of problems dealing with conduction and radiation heat transfer. All previous studies [9–15] of the LBM applied to heat transfer problems dealt with constant thermophysical properties and the method was found to provide accurate results.

In most heat transfer problems, temperature varies over a wide range. Ideally, thermal conductivity of the medium is temperature dependent, and in such problems, the assumption of constant thermal conductivity provides less accurate results [16–19]. However, with consideration of temperature dependent thermal conductivity, the energy equation becomes nonlinear and its solution thus becomes difficult [16–19].

To extend the usage of the LBM to account for variable thermophysical properties, the present work is aimed at providing a new formulation of the LBM to deal with temperature dependent thermal conductivity. With variable thermal conductivity, unlike the case of constant properties, the relaxation time in the LBM becomes temperature dependent, and this concept of variable relaxation time has not yet been studied.

A large class of problems involves analysis of conduction and radiation heat transfer. In such problems, to provide the radiative information for the energy equation, the discrete ordinates method (DOM) [20] is one of the most widely used methods. Another objective of the present work, therefore, is also to show the numerical compatibility of two different kinds of methods, the LBM and the DOM.

To validate the formulation, one-dimensional transient heat conduction without radiation in a planar medium with temperature-dependent thermal conductivity has been considered first. Next, the LBM has been applied to solve the energy equation of problems involving one-dimensional conduction and radiation heat transfer with temperature-dependent thermal conductivity. To check the suitability of the LBM, the energy equation of the same problems has also been solved using the FDM. The DOM has been used in both cases to find the radiative information. For benchmarking purposes, some sample results have been compared with those available in the literature [16,18]. Comparisons of the number of iterations and CPU times in the two methods have also been made.

II. Formulation

Consider a one-dimensional planar absorbing, emitting, and scattering medium (Fig. 1). Thermophysical properties such as density, specific heat, and extinction coefficient are assumed to be constant. Initially the entire system is at temperature T_E, and for time $t > 0$, the west boundary is maintained at temperature T_W. The thermal conductivity of the medium is assumed to vary with temperature. Its variation is given by

$$k = k_0 + \gamma'(T - T_W) \tag{1}$$

where k_0 is the reference thermal conductivity. In the absence of convection and heat generation, for the problem under consideration, the energy equation is given by

$$\rho c_P \frac{\partial T}{\partial t} = -\frac{\partial}{\partial x}\left(-k\frac{\partial T}{\partial x}\right) - \frac{\partial q_R}{\partial x} \tag{2}$$

Substituting for k from Eq. (1) into Eq. (2), we get

$$\rho c_P \frac{\partial T}{\partial t} = [k_0 + \gamma'(T - T_W)]\frac{\partial^2 T}{\partial x^2} + \gamma'\left(\frac{\partial T}{\partial x}\right)^2 - \frac{\partial q_R}{\partial x} \tag{3}$$

With nondimensional temperature, distance x^*, conduction-radiation parameter, radiative heat flux Ψ_R, time ξ, and variable thermal conductivity parameter defined in the following way

$$\theta = \frac{T}{T_W} \qquad x^* = \beta x \qquad N = \frac{k_0\beta}{4\sigma T_W^3} \qquad \Psi_R = \frac{q_R}{\sigma T_W^4}$$
$$\xi = \alpha\beta^2 t \qquad \gamma = \frac{\gamma' T_W N}{k_0} \tag{4}$$

Eq. (3) becomes

$$\frac{\partial\theta}{\partial\xi} = \left(1 + \frac{\gamma(\theta-1)}{N}\right)\frac{\partial^2\theta}{\partial x^{*2}} + \frac{\gamma}{N}\left(\frac{\partial\theta}{\partial x^*}\right)^2 - \frac{1}{4N}\frac{\partial\Psi_R}{\partial x^*} \tag{5}$$

For the problem under consideration, the initial and boundary conditions are the following:

Initial condition

$$T(x, 0) = T_E \tag{6}$$

Boundary conditions

$$T(0, t) = T_W, \qquad T(X, t) = T_E$$

Equation (5) is a nonlinear partial differential equation in which, apart from the nonlinearity in the radiative term $\partial\Psi_R/\partial x^*$, the first two terms on the right-hand side are also nonlinear. While solving the energy equation of any radiation, conduction, and/or convection mode problems, at any time level, radiative information is calculated from the temperature values of the previous iteration. Thus, the nonlinearity in the overall energy equation, as caused by radiation, does not appear. However, nonlinearity in other terms of the energy equation requires separate treatment whose solution in the conventional CFD methods such as the FDM is complicated. Details on the solution of Eq. (5) using the FDM can be found in [16–19]. In the LBM, however, solution of this problem is simpler. In the

following pages, we first provide a brief formulation of the DOM to compute the radiative information $\partial q_R/\partial x$ and then discuss the LBM to solve the energy equation.

A. Discrete Ordinates Method Formulation

The divergence of the radiative heat flux $\partial q_R/\partial x$ is given by [20]

$$\frac{\partial q_R}{\partial x} = \kappa_a\left(4\pi\frac{\sigma T^4}{\pi} - G\right) \tag{7}$$

which, for a planar medium, is given by the following form and from [21]

$$G = 2\pi\int_{\theta}^{\pi} I(\delta)\sin\delta\,\mathrm{d}\delta \approx 4\pi\sum_{m=1}^{M} I(\delta^m)\sin\delta^m\sin\left(\frac{\Delta\delta^m}{2}\right) \tag{8}$$

where M is the total number of intensities I considered over the complete span of $\delta(0 \le \delta \le \pi)$.

In the DOM, for a planar medium, the radiative transfer equation for the discrete direction m is given by

$$\mu^m\frac{\partial I^m}{\partial x} = -\beta I^m + S^m \tag{9}$$

where $\mu = \cos\delta$ is the direction cosine. For a planar medium S is given by

$$S = \frac{\kappa_a\sigma T^4}{\pi} + \frac{\sigma_s}{4\pi}2\pi\int_0^{\pi} I(\delta)\Phi(\delta,\delta')\sin\delta\,\mathrm{d}\delta \tag{10}$$

where Φ is the anisotropic phase function. If the medium is absorbing, emitting, and isotropically scattering ($\Phi = 1$), the source term can be written as

$$S = \kappa_a\frac{\sigma T^4}{\pi} + \frac{\sigma_S}{4\pi}G \tag{11}$$

Integrating Eq. (9) over a one-dimensional control volume, we get

$$\mu^m\left(I_E^m - I_W^m\right) = -\beta dx I_P^m + dx S_P^m \tag{12}$$

where I_E and I_W are the intensities at the east and the west cell boundaries, and I_P and S_P are the intensity and the source term at the cell center P. If $I_P = (I_E + I_W)/2$, in terms of known intensities, the cell center intensity I_P can be written as

$$I_p^m = \begin{cases} \frac{2\mu^m I_W^m + S_p^m dx}{2\mu^m + \beta dx}, & \mu > 0 \\ \frac{2|\mu^m| I_E^m + S_p^m dx}{2|\mu^m| + \beta dx}, & \mu < 0 \end{cases} \tag{13}$$

In the preceding equations, δ has been measured clockwise from the outward normal to the west boundary. Marching from the west boundary we have $\mu > 0$ and I_W is the known intensity in a given control volume. For a boundary control volume, the unknown intensity is found from the radiative boundary condition. For a diffuse-gray boundary with emissivity ε_b and temperature T_b, boundary intensity $I_{b=E,W}$ is computed from [21]

$$I_{b=E,W} = \frac{\varepsilon_b\sigma T_b^4}{\pi} + \left(\frac{1-\varepsilon_b}{\pi}\right)2\pi\sum_{m=1}^{M/2} I^m\cos\delta^m\sin\delta^m\sin(\Delta\delta^m) \tag{14}$$

Once the intensities are known, radiative heat flux can be computed from the following [21]

$$q_R = 2\pi\int_{\delta=0}^{\pi} I(\delta)\cos\delta\sin\delta\,\mathrm{d}\delta \approx 2\pi\sum_{m=1}^{M} I^m\cos\delta^m\sin\delta^m\sin(\Delta\delta^m) \tag{15}$$

and the divergence of radiative heat flux required for the energy equation is computed from Eq. (7).

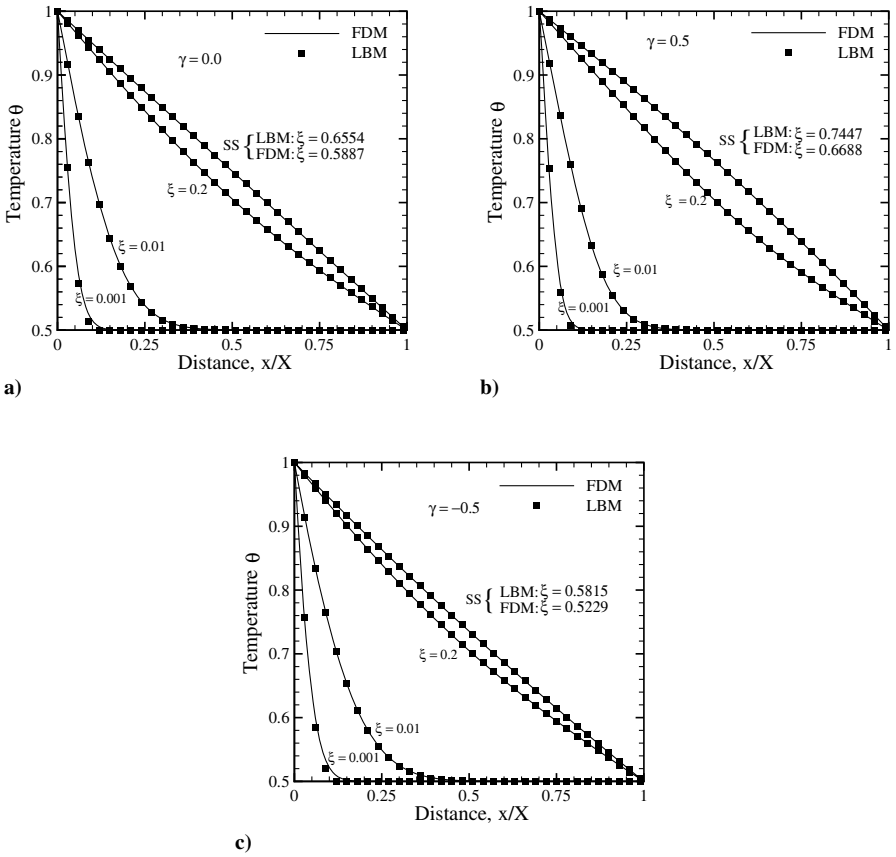

Fig. 2 Comparison of θ at different instants of ξ for one-dimensional conduction problem without radiation.

Table 1 Comparison of steady-state nondimensional heat flux results [16,18]; $N = 0.5$, $\beta = 1.0$, $\theta_E = 0.5$

ω	γ	x/X	Chu and Tseng [16]		Talukdar and Mishra [18]		Present work			
							FDM-DOM		LBM-DOM	
			$\Psi_C/4$	$\Psi_R/4$	$\Psi_C/4$	$\Psi_R/4$	$\Psi_C/4$	$\Psi_R/4$	$\Psi_C/4$	$\Psi_R/4$
0.0	0.4	0.25	0.3791	0.1645	0.3791	0.1644	0.3802	0.1641	0.3801	0.1641
		0.50	0.3876	0.1559	0.3876	0.1559	0.3885	0.1555	0.3885	0.1555
		0.75	0.4138	0.1298	0.4138	0.1297	0.4141	0.1293	0.4142	0.1293
0.0	−0.4	0.25	0.0739	0.1668	0.0739	0.1668	0.0743	0.1665	0.0741	0.1665
		0.50	0.0917	0.1491	0.0917	0.1490	0.0918	0.1484	0.0917	0.1485
		0.75	0.1203	0.1204	0.1203	0.1204	0.1197	0.1198	0.1201	0.1199
0.5	0.4	0.25	0.3858	0.1520	0.3858	0.1520	0.3871	0.1516	0.3870	0.1517
		0.50	0.3925	0.1453	0.3924	0.1454	0.3932	0.1450	0.3932	0.1450
		0.75	0.4101	0.1277	0.4101	0.1277	0.4101	0.1274	0.4102	0.1275
0.5	−0.4	0.25	0.0810	0.1550	0.0809	0.1551	0.0813	0.1548	0.0809	0.1548
		0.50	0.0952	0.1408	0.0951	0.1409	0.0950	0.1404	0.0950	0.1405
		0.75	0.1157	0.1203	0.1157	0.1203	0.1150	0.1198	0.1154	0.1199

B. Lattice Boltzmann Method Formulation

The starting point of the LBM is the kinetic equation which for a one-dimensional geometry with the D1Q2 lattice (Fig. 1) is given by [3,4,13]

$$\frac{\partial f_i(\boldsymbol{x},t)}{\partial t} + \boldsymbol{e}_i \cdot \nabla f_i(\boldsymbol{x},t) = \Omega_i \qquad i = 1 \text{ and } 2 \tag{16}$$

where f_i denotes the number of particles at the lattice node $\boldsymbol{x}$ and t moving in direction i with velocity $\boldsymbol{e}_i$ along the lattice link $\Delta x = e_i \Delta t$ connecting the neighbors. The discrete Boltzmann equation with the Bhatanagar–Gross–Krook (BGK) approximation [22] is given by [3,4]

$$\frac{\partial f_i(\boldsymbol{x},t)}{\partial t} + \boldsymbol{e}_i \cdot \nabla f_i(\boldsymbol{x},t) = -\frac{1}{\tau}\left[f_i(\boldsymbol{x},t) - f_i^{(0)}(\boldsymbol{x},t)\right] \tag{17}$$

For a given application, relaxation time is different for different lattices. In the present work, for a one-dimensional planar medium, the relaxation time for the D1Q2 lattice (Fig. 1) is computed from [3,4]

$$\tau = \frac{\alpha}{|\boldsymbol{e}_i|^2} + \frac{\Delta t}{2} \tag{18}$$

For this lattice, the two velocities e_1 and e_2, and their corresponding weights w_1 and w_2 are given by

$$e_1 = \frac{\Delta x}{\Delta t}, \qquad e_2 = -\frac{\Delta x}{\Delta t} \tag{19}$$

$$w_1 = w_2 = \frac{1}{2} \tag{20}$$

It is to be noted that for any kind of lattice, weights always satisfy the relation

$$\sum_{i=1}^{m} w_i = 1 \tag{21}$$

After discretization, Eq. (17) can be written as [3,4]

$$f_i(\boldsymbol{x} + \boldsymbol{e}_i \Delta t, t + \Delta t) = f_i(\boldsymbol{x},t) - \frac{\Delta t}{\tau}\left[f_i(\boldsymbol{x},t) - f_i^{(0)}(\boldsymbol{x},t)\right] \tag{22}$$

Equation (22) is the LBM equation with the BGK approximation that describes the evolution of the particle distribution function. The algorithm for Eq. (22) can be divided into two essential parts per time step:

1) The calculation of new distribution functions with respect to the right-hand side of Eq. (22), the so-called collision.

2) The streaming of the distribution functions to the next neighboring nodes usually referred to as propagation.

In the case of heat transfer problems, the temperature is obtained after summing f_i over all directions [3,4,13], i.e.,

$$T(\boldsymbol{x},t) = \sum_{i=1,2} f_i(\boldsymbol{x},t) \tag{23}$$

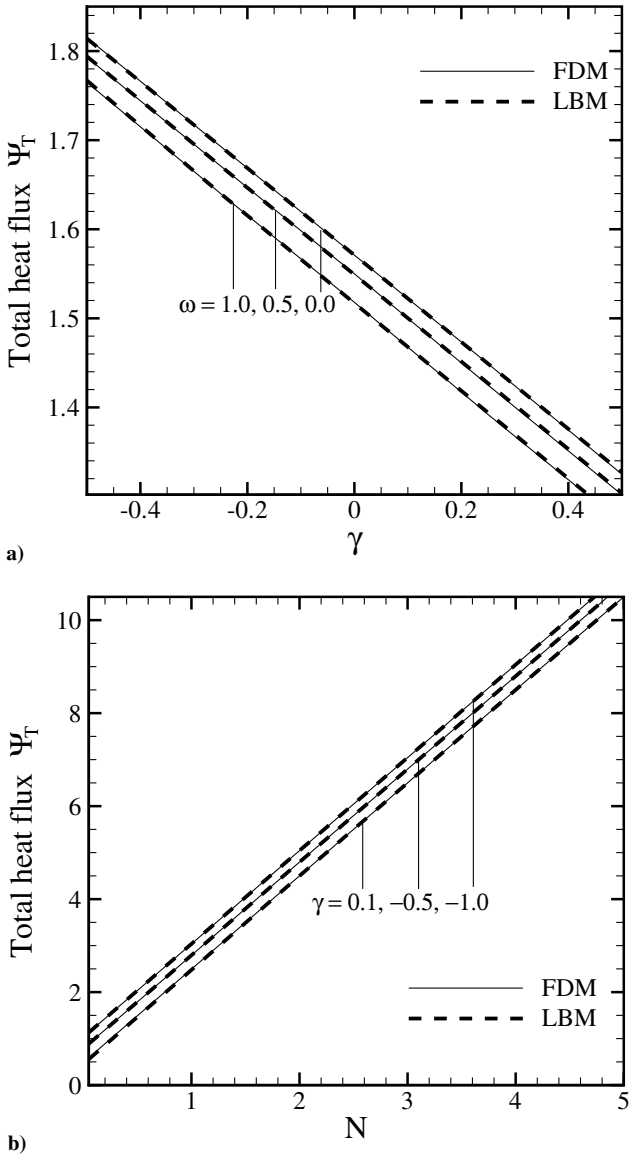

Fig. 3 Comparison of variation of Ψ_T.

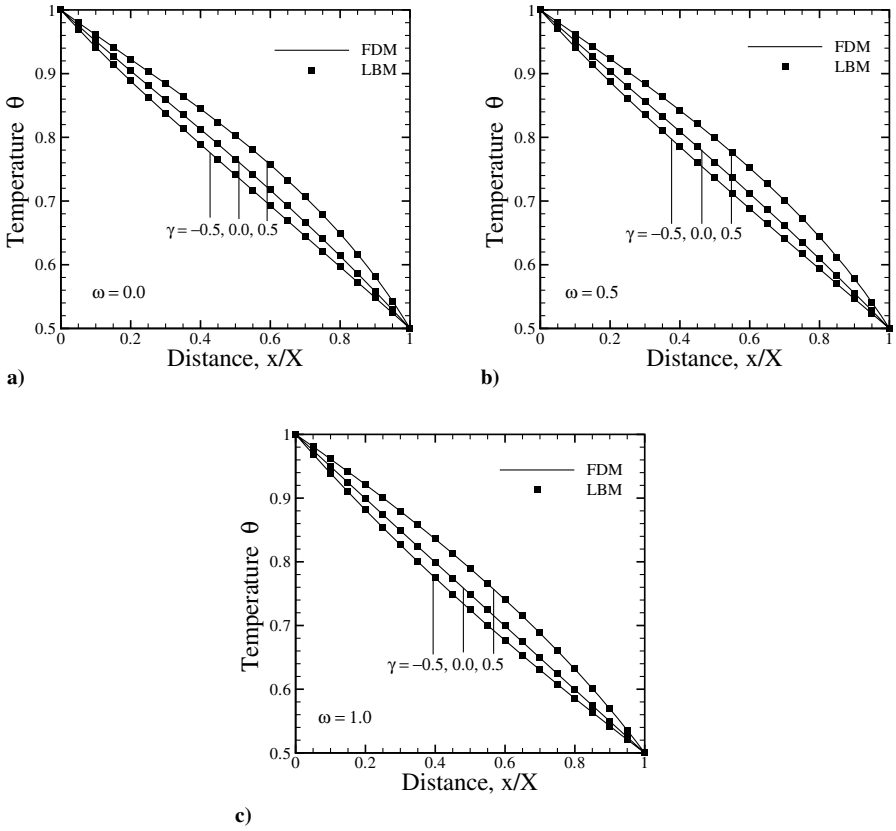

Fig. 4 Comparison of θ for different values of γ for scattering albedo.

To process Eq. (22), an equilibrium distribution function is required. For heat conduction problems, this is given by

$$f_i^{(0)}(\boldsymbol{x}, t) = w_i T(\boldsymbol{x}, t) \tag{24}$$

From Eqs. (21), (23), and (24), we also have

$$\sum_{i=1,2} f_i^{(0)}(\boldsymbol{x}, t) = \sum_{i=1,2} w_i T(\boldsymbol{x}, t) = T(\boldsymbol{x}, t) = \sum_{i=1,2} f_i(\boldsymbol{x}, t) \tag{25}$$

Equation (25), with definitions of temperature $T(\boldsymbol{x}, t)$ and equilibrium distribution function $f_i^{(0)}(\boldsymbol{x}, t)$ given in Eqs. (23) and (24), respectively, provide the solution of a transient heat conduction problem in the LBM. To account for the radiation term (term 3) in the energy equation [Eq. (3)], in the LBM formulation, Eq. (22) is modified to [11,12]

$$f_i(\boldsymbol{x} + \boldsymbol{e}_i \Delta t, t + \Delta t) = f_i(\boldsymbol{x}, t) - \frac{\Delta t}{\tau}\left[f_i(\boldsymbol{x}, t) - f_i^{(0)}(\boldsymbol{x}, t)\right] - \frac{\Delta t w_i}{\rho c_p}\frac{\partial q_R}{\partial x} \tag{26}$$

Equation (26) is the equivalent form of the energy equation [Eq. (3)] in the LBM formulation.

To account for the temperature dependent thermal conductivity [Eq. (1)], the expression for the relaxation time given in Eq. (18) is modified as

$$\tau = \frac{k/\rho c_p}{|\boldsymbol{e}_i|^2} + \frac{\Delta t}{2} = \frac{k_0 + \gamma'(T - T_W)}{\rho c_p |\boldsymbol{e}_i|^2} + \frac{\Delta t}{2} = \frac{k_0}{\rho c_p |\boldsymbol{e}_i|^2} + \frac{\gamma'}{\rho c_p |\boldsymbol{e}_i|^2}(T - T_W) + \frac{\Delta t}{2} \tag{27}$$

With nondimensional quantities as defined in Eq. (4), Eq. (26) in nondimensional form is given by

$$f_i^*(\boldsymbol{x}^* + \boldsymbol{e}_i^* \Delta\xi, \xi + \Delta\xi) = f_i^*(\boldsymbol{x}^*, \xi) - \frac{\Delta t}{\tau^*}[f_i(\boldsymbol{x}^*, \xi) - f_i^{*(0)}(\boldsymbol{x}^*, \xi)] - \frac{\Delta\xi w_i}{4N}\frac{\partial \Psi_R}{\partial x^*} \tag{28}$$

where the divergence of radiative heat flux in nondimensional form is

$$\frac{\partial \Psi_R}{\partial x^*} = 4(1 - \omega)\left(\theta^4 - \frac{G^*}{4\pi}\right) \tag{29}$$

and the relaxation time has the following form

$$\tau^* = \frac{1}{(\Delta x^*/\Delta\xi)^2} + \frac{\gamma}{(\Delta x^*/\Delta\xi)^2}(\theta - \theta_W) + \frac{\Delta\xi}{2} \tag{30}$$

In the LBM, at the boundaries, the particle distribution functions going inside the medium (Fig. 1) are unknown and these are computed from the boundary conditions. For the present problem, at the west and the east boundaries, the unknown particle distribution functions $f_1^*(0, \xi)$ and $f_2^*(\beta X, \xi)$ are given by

(at the west boundary)

$$f_1^*(0, \xi) = -f_2^*(0, \xi) + \theta_W \tag{31}$$

(at the east boundary)

$$f_2^*(\beta X, \xi) = -f_1^*(\beta X, \xi) + \theta_E$$

Details on implementation of the temperature as well as flux boundary conditions for various geometries are given in [13] and the solution procedure in the LBM to solve conduction-radiation problems can be found in [11,12].

III. Results and Discussion

The LBM formulation with variable thermal conductivity presented in the preceding section is validated first by solving

a one-dimensional transient heat conduction problem without radiation. Next, we consider transient conduction and radiation heat transfer in an absorbing, emitting, and scattering planar layer. Both with and without radiation, the governing energy equation was also solved using the FDM [16]. In both the methods, radiative information was computed using the DOM. In solving these problems, for the grid independent situation, 100 lattices (control volumes in the FDM and the DOM) were used. For the ray independent situation, 16 equally spaced discrete directions were used in the DOM. The direction cosines and the procedure for the evaluation of incident radiation and heat flux were based on the procedure suggested in [21] and as given in Eqs. (8) and (15). Steady-state (SS) conditions in both the LBM and the FDM were assumed to have been reached when the temperature difference between two consecutive time levels at each lattice center (node in the FDM) did not exceed 1×10^{-6}. In solving the energy equation, a nondimensional time step of $\Delta\xi = 0.0001$ was considered. For all of the cases (with or without radiation) considered, the initial and the boundary conditions are given in Eq. (6) in which $T_W = 2T_E$.

A. One-Dimensional Heat Conduction Without Radiation

Nondimensional temperature results for one-dimensional transient heat conduction without radiation for the variable thermal conductivity parameter have been presented in Fig. 2. For $\gamma = 0.0$, 0.5, and -0.5, θ at different instants of time ξ obtained from the LBM has been compared with the FDM results in Figs. 2a–2c, respectively. It can be seen from Fig. 2 that for all values of γ, the SS results of the two methods match very well with each other. However, because the convergence rates of the two methods are not the same [11,12], transient results of the two methods differ slightly at some values of ξ. The SS time of the LBM is seen to be greater than that of the FDM.

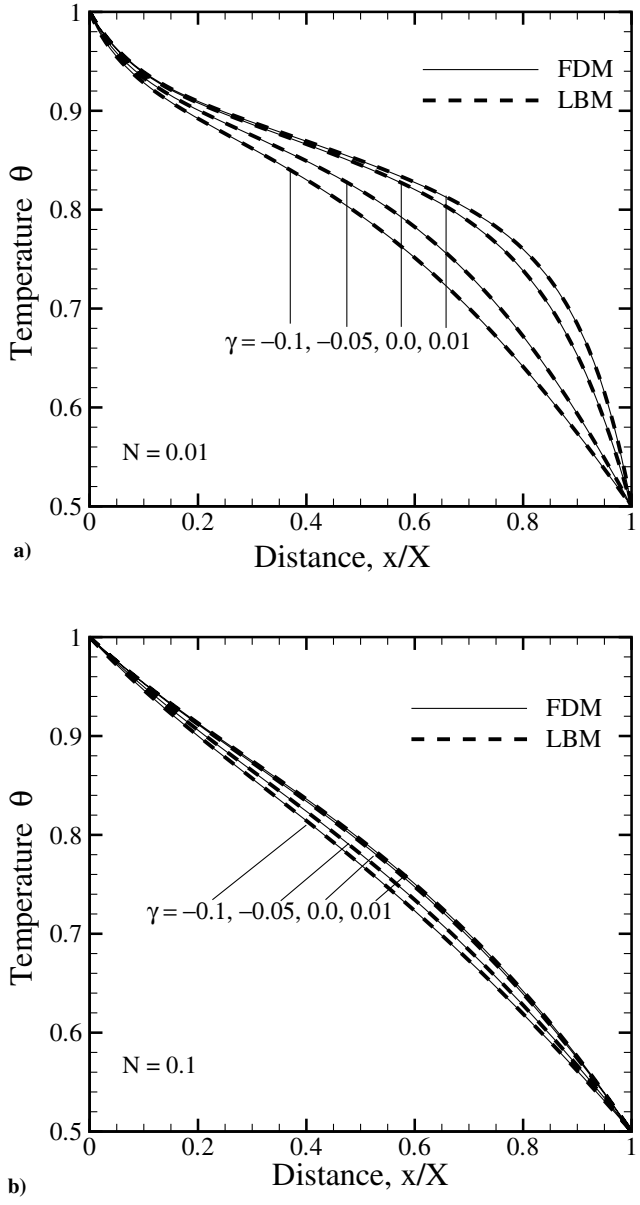

Fig. 5 Comparison of θ for different values of γ for N.

B. One-Dimensional Heat Conduction with Radiation

In the following pages, the SS results are presented for one-dimensional transient conduction and radiation heat transfer. Radiatively, the homogeneous and gray medium has been taken as absorbing, emitting, and isotropically scattering, and both boundaries have been considered black.

In Table 1, the nondimensional SS heat flux results of the LBM and the FDM using the DOM for the radiative information have been validated with Chu and Tseng [16], and Talukdar and Mishra [18]. For the conduction-radiation parameter $N = 0.5$, the extinction coefficient $\beta = 1.0$, and $\theta_E = 0.5$, the conductive heat flux Ψ_C and the radiative heat flux Ψ_R have been compared at three different locations in the medium. For scattering albedo $\omega = 0$ and 0.5, these comparisons have been made for the two values of the coefficient of thermal conductivity variation, viz., 0.4 and -0.4. It is to be noted that to compare this work with that of [16,18], we have taken the thermal conductivity variation here as $k = k_0 + \gamma' T$. However, for the rest of the results, the thermal conductivity variation is given by Eq. (1). It can be seen from Table 1 that the LBM and the FDM results compare very well with those of [16,18].

It is to be noted that for the results in Table 1 and in the following pages, at any location in the medium, including the two boundaries, the conductive heat flux Ψ_C and the total flux Ψ_T have been

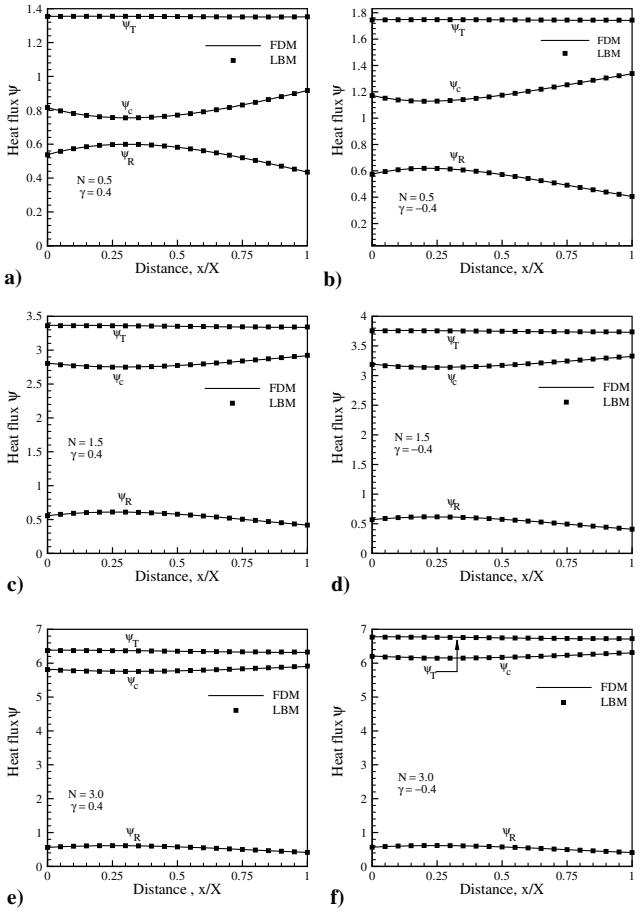

Fig. 6 Comparison of Ψ_T, Ψ_C, and Ψ_R; $\beta = 1.0$, $\omega = 0.5$.

Table 2 Comparison of iterations and CPU time; DOM was used to compute radiativity

Coefficient of thermal conductivity variation γ	Conduction-radiation parameter N	LBM		FDM	
		Iterations	CPU time, s	Iterations	CPU time, s
−0.5	0.1	2465	1.156	2404	1.172
−0.5	2.0	5812	2.906	5451	2.750
−0.5	5.0	6010	3.046	5665	2.812
0.5	0.5	7316	3.687	6892	3.485
0.0	0.5	5647	2.828	5454	2.765
−0.5	0.5	4704	2.360	4516	2.230

computed from

$$\Psi_T = \Psi_C + \Psi_R = -4N\left[1 + \frac{\gamma}{N}(\theta - 1)\right]\frac{d\theta}{dx^*} + \Psi_R \qquad (32)$$

Having validated the results of the FDM and the LBM with those available in the literature, results of the two methods are now compared with each other for different situations.

In Fig. 3a, for the conduction-radiation parameter $N = 0.5$, the total heat flux Ψ_T results of the LBM and the FDM have been compared for variation of the coefficient of thermal conductivity for three different values of the scattering albedo. In Fig. 3b, for $\omega = 0.5$, the same have been compared for variation of N for three different values of γ. For results in Figs. 3a and 3b, the extinction coefficient $\beta = 1.0$. It can be seen from Fig. 3 that the LBM results and the FDM results are in very good agreement with each other.

With $N = 0.5$ and $\beta = 1.0$, for $\gamma = -0.5$, 0.0, and 0.5, temperature results of the LBM and the FDM have been compared for $\omega = 0.0$, 0.5, and 1.0 in Figs. 4a–4c, respectively. The LBM and the FDM results are seen to perfectly match with each other. For all values of ω, γ is seen to have a significant effect on θ. However, for a given value of γ, the variation of θ with ω is not significant.

In Figs. 5a and 5b, θ variation has been compared for $N = 0.01$ and 0.1, respectively. In both of the figures, θ variations have been compared for the four different values of γ. For these results, $\beta = 1.0$ and $\omega = 0.5$. In the radiation dominated situation (Fig. 5a), γ is seen to have a significant effect on θ, and this effect is close to the east (colder) boundary. The LBM and the FDM results are seen to compare very well with each other.

For $\beta = 1.0$ and $\omega = 0.0$, in Figs. 6a–6f, the total heat flux Ψ_T, the conductive heat flux Ψ_C, and the radiative heat flux Ψ_R, have been compared for different values of N and γ. In these figures, comparisons have been shown for $N = 0.5$, 1.5, and 3.0, and $\gamma = 0.4$ and -0.4. With an increase in the value of N, the situation becomes more conduction dominated, and accordingly the contribution of Ψ_C to Ψ_T is seen to increase. Although Ψ_C and Ψ_R continuously vary inside the medium, as expected, their sum Ψ_T is constant at every point in the medium. The LBM and the FDM results are seen to compare exactly with each other.

C. Comparison of CPU Times and Number of Iterations

To get an idea of the CPU times (in seconds) and the number of iterations in the LBM and the FDM, some results are presented in Table 2. All runs were made on an IBM Thinkpad, model R40, Mobile Intel Pentium 4, 2.0 GHz, 256 MB RAM at 266 MHz. With $\beta = 1.0$ and $\omega = 0.5$, for three values of γ and three values of N, the CPU times and the number of iterations have been compared for 100 lattices/control volumes and 16 directions in the DOM. For a given value of $\gamma = -0.5$, in the radiation dominated situation (lower values of N), both methods converge fast and LBM is faster than the FDM. However, in the conduction dominated case, FDM is faster than the LBM. Further, it is seen that for a given value of N, both methods converge fast for the negative values of γ and the LBM is seen to take more iterations. For $\gamma < 0$, the second term on the right-hand side of Eq. (1) is always positive (because T_W is always greater than T). Thus, the lower the value of γ, the higher the value of thermal conductivity and, subsequently, the faster is the convergence to SS.

IV. Conclusions

The LBM was applied to solve the energy equation for problems dealing with variable thermal conductivity which was assumed to vary linearly with temperature. In all cases, to compare the performance of the LBM, the energy equation was also solved using the FDM. Radiative information from both methods was computed using the DOM. In all cases, the LBM was found to provide accurate results. In most cases, for the SS solutions, the LBM was found to take more iterations and the CPU time was slightly higher than that for the FDM.

The basic objective of the present work was to emphasize the concept of variable relaxation time τ [Eq. (27)] and to highlight the applicability of the LBM to deal with variable thermal conductivity problems with ease and accuracy. In addition, the work also highlighted the numerical compatibility of two different kinds of methods, the LBM and the DOM. The LBM was found to work very well for all cases considered. In multidimensional geometries with greater complexity, like hydrodynamics, computationally the LBM may have an advantage over conventional methods. Hence, the usage of the LBM for complex thermofluid problems with or without radiation should be explored.

References

[1] Chen, S., and Doolen, G. D., "Lattice Boltzmann Method for Fluid Flows," *Annual Review of Fluid Mechanics*, Vol. 30, No. 1, 1998, pp. 329–364.

[2] He, X., Chen, S., and Doolen, G. D., "A Novel Thermal Model for the Lattice Boltzmann Method in Incompressible Limit," *Journal of Computational Physics*, Vol. 146, No. 1, 1998, pp. 282–300.

[3] Wolf-Gladrow, D. A., *Lattice-Gas Cellular Automata and Lattice Boltzmann Models: An Introduction*, Springer–Verlag, Berlin, 2000.

[4] Succi, S., *The Lattice Boltzmann Method for Fluid Dynamics and Beyond*, Oxford Univ. Press, Oxford, England, U.K., 2001.

[5] Nourgaliev, R. R., Dinh, T. N., Theofanous, T. G., and Joseph, D. "The Lattice Boltzmann Equation Method: Theoretical Interpretation, Numerics and Implications," *International Journal of Multiphase Flow*, Vol. 29, No. 1, 2003, pp 117–169.

[6] Zhu, L., Tretheway, D., Petzold, L., and Meinhart, C., "Simulation of Fluid Slip at 3D Hydrophobic Micro Channel Walls by the Lattice Boltzmann Method," *Journal of Computational Physics*, Vol. 202, No. 1, 2005, pp. 181–195.

[7] Xi, H., Peng, G., and Chou, S.-H., "Finite-Volume Lattice Boltzmann Schemes in Two and Three Dimensions," *Physical Review E (Statistical Physics, Plasmas, Fluids, and Related Interdisciplinary Topics)*, Vol. 60, No. 3, 1999, pp. 3380–3388.

[8] Takada, N., Misawa, M., Tomiyama, A., and Fujiwara, S., "Numerical Simulation of Two- and Three-Dimensional Two-Phase Fluid Motion by Lattice Boltzmann Method," *Computer Physics Communications*, Vol. 129, No. 1, 2000, pp. 233–246.

[9] Ho, J. R., Kuo, C.-P., and Jiaung, W. S., "Study of Heat Transfer in Multilayered Structure Within the Framework of Dual-Phase-Lag Heat Conduction Model Using Lattice Boltzmann Method," *International Journal of Heat and Mass Transfer*, Vol. 46, No. 1, 2003, pp. 55–69.

[10] Ho, J. R., Kuo, C.-P., and Jiaung, W.-S., and Twu, C.-J., "Lattice Boltzmann Scheme for Hyperbolic Heat Conduction Equation," *Numerical Heat Transfer: Part B, Fundamentals*, Vol. 41, No. 6, 2002, pp. 591–607.

[11] Mishra, S. C., and Lankadasu, A.,"Transient Conduction-Radiation Heat Transfer in Participating Media Using the Lattice Boltzmann Method and the Discrete Transfer Method," *Numerical Heat Transfer: Part A, Applications*, Vol. 47, No. 9, 2005, pp. 935–954.

[12] Mishra, S. C., Lankadasu, A., and Beronov, K., "Application of the Lattice Boltzmann Method for Solving the Energy Equation of a 2-D Transient Conduction-Radiation Problem," *International Journal of Heat and Mass Transfer*, Vol. 48, No. 17, 2006, pp. 3648–3659.

[13] Kush, T., Krishna, B. S. R., and Mishra, S. C., "Comparisons of the Lattice Boltzmann Method and the Finite Difference Methods for Heat Conduction Problems," *Proceedings of 18th National & 7th ISHMT-ASME Heat and Mass Transfer Conference*, edited by S. C. Mishra, BVSSS Prasad, and S. V. Garimella, Paper HMT-2006-C012, McGraw–Hill, New Delhi, India, 2006.

[14] Jiaung, W.-S., Ho, J. R., and Kuo, C.-P., "Lattice Boltzmann Method for Heat Conduction Problem with Phase Change," *Numerical Heat Transfer: Part B, Fundamentals*, Vol. 39, No. 2, 2001, pp. 167–187.

[15] Raj, R., Prasad, A., Parida, P. R., and Mishra, S. C., "Analysis of Solidification of a Semitransparent Planar Layer Using the Lattice Boltzmann Method and the Discrete Transfer Method," *Numerical Heat Transfer: Part A, Applications*, Vol. 49, No. 3, 2006, pp. 279–299.

[16] Chu, H. S., and Tseng, C. J., "Conduction-Radiation Interaction in Absorbing, Emitting and Scattering Media with Variable Thermal Conductivity," *Journal of Thermophysics and Heat Transfer*, Vol. 6, No. 3, 1992, pp. 537–540.

[17] Tseng, C. J., and Chu, H. S., "Transient Combined Conduction and Radiation in an Absorbing, Emitting and Anisotropically Scattering Medium with Variable Thermal Conductivity," *International Journal of Heat and Mass Transfer*, Vol. 35, No. 7, 1992, pp. 1844–1847.

[18] Talukdar, P., and Mishra, S. C., "Transient Conduction and Radiation Heat Transfer with Variable Thermal Conductivity," *Numerical Heat Transfer: Part A, Applications*, Vol. 41, No. 8, 2002, pp. 851–867.

[19] Mishra, S. C., Talukdar, P., Trimis, D., and Durst, F., "Two-Dimensional Transient Conduction and Radiation Heat Transfer with Variable Thermal Conductivity," *International Communications in Heat and Mass Transfer*, Vol. 32, Nos. 3–4, 2005, pp. 305–314.

[20] Modest, M. F., *Radiative Heat Transfer*, 2nd ed., Academic Press, New York, 2003.

[21] Mishra, S. C., Misra, N., and Roy, H. K., "Discrete Ordinate Method with a New and a Simple Quadrature Scheme," *Journal of Quantitative Spectroscopy and Radiative Transfer*, Vol. 101, No. 2, 2006, pp. 249–262 (to be published).

[22] Bhatanagar, P., Gross, E. P., and Krook, M. K., "A Model for Collision Processes in Gases, Part 1: Small Amplitude Processes in Charged and Neutral One-Component Systems," *Physical Review*, Vol. 94, No. 3, 1954, pp. 511–525.